Published in final edited form as:
Curr Biol. 2010 June 8; 20(11): 989–993. doi:10.1016/j.cub.2010.03.064.

Loss of INCREASED SIZE EXCLUSION LIMIT (ISE)1 or ISE2 increases the formation of secondary plasmodesmata

Tessa M. Burch-Smith and **Patricia C. Zambryski**[1]
Department of Plant and Microbial Biology, Koshland Hall, University of California, Berkeley, CA 94720

Summary

Plasmodesmata (PD) transport developmentally important nucleic acids and proteins between plant cells [1,2,3]. Primary PD form during cell division and are simple, linear channels [4,5]. Secondary PD form in existing cell walls post cell division and are simple, twinned or branched [4]. PD function undergoes a marked reduction at the mid-torpedo stage of *Arabidopsis* embryogenesis [6]. Two mutants, *increased size exclusion limit* (*ise*)*1* and *ise2*, fail to undergo this transition, and their null mutations are embryo lethal [7,8]. We investigated the ultrastructure of PD in early, mid, and late torpedo-staged embryos and in young leaves. Wild type (WT) embryos contain twinned/branched (T/B) PD at all stages but *ise1* and *ise2* embryos contain significantly higher proportions of T/B PD than WT embryos. WT T/B PD formation occurs in a stage and tissue-specific pattern that is reversed in *ise1* embryos. Silencing *ISE1* in *Nicotiana benthamiana* leaves increases the frequency of secondary PD in existing cell walls. Silencing *ISE2* increases the proportion of T/B secondary PD formed. Silenced tissues exhibit increased PD-mediated movement of GFP tracers. Thus silencing of *ISE1* and *ISE2* phenocopies *ise1* and *ise2* mutant embryos: when wild type ISE1 and ISE2 functions are lost de novo production of PD occurs leading to increased intercellular transport.

Results and Discussion

PD function correlates with increased twinned and branched PD in *ise1* and *ise2* embryos

ise1 and *ise2* embryos fail to undergo the mid-torpedo stage specific reduction in PD transport [6,7,8]. To determine if PD structural changes explain WT or mutant phenotypes we examined PD of early, mid and late torpedo-stage WT, *ise1* and *ise2 Arabidopsis* embryos by TEM. Figure S1 shows the morphology of the embryos analyzed. Simple PD typically associated with immature tissues were observed in all stages (Fig. 1A). We also observed PD with more

[1] To whom correspondence should be addressed: zambrysk@berkeley.edu, Tel. No: 510-643-9203.

Highlights:

1. *Arabidopsis* torpedo-stage embryos contain T/B PD.
2. T/B PD formation is genetically regulated.
3. Increased T/B PD formation correlates with increased intercellular transport in *ise1* and *ise2* embryos.
4. Reduced *ISE1* and/or *ISE2* transcript levels increase secondary PD formation and intercellular transport.

Accession numbers: NbISE2 sequence is deposited at the GenBank database under the accession number 1317874.

complex structures including twinned (T), defined as two PD less than 100 nm apart (Fig. 1B), and branched (B) PD (Fig. 1C-D). For simplicity, we refer to all non-simple PD as T/B PD.

We scored at least 100 PD in a minimum of two non-serial longitudinal sections of cotyledons or hypocotyls of early, mid or late torpedo-stage WT, *ise1*, and *ise2* embryos (Table S1). Figure S1 exemplifies the quality of the images analyzed. Figure 1E shows first that WT torpedo-staged embryos contain T/B PD. A previous study [7] did not detect T/B PD in WT embryos, presumably because few PD were assayed while here we analyzed 860 WT PD. Second, there is no change in the T/B-PD frequency between early and mid-torpedo stages in WT embryos. Thus, decreased transport in WT mid-torpedo embryos may result from a mechanism for regulating transport that does not detectably alter PD structure. Third, in all stages examined, *ise1* and *ise2* mutants display significantly larger proportions of T/B PD than sibling WT embryos. These data suggest that the increased intercellular transport observed in *ise1* and *ise2* is due to increased T/B-PD formation.

In WT embryos the hypocotyl contains more T/B PD than the cotyledon in early and mid-torpedo embryos, but this distribution is reversed in late-torpedo embryos (Fig. 1E, black bars). *ise2* mutant embryos show a similar pattern of T/B PD formation (Fig. 1E, grey bars). Strikingly, in *ise1* mutant embryos this pattern is exactly reversed (Fig. 1E, white bars). Thus, T/B-PD formation is under the control of a specific, developmentally regulated program, and loss of *ISE1* critically affects the pathway that determines when and where T/B PD form.

Strategy to assess primary and secondary PD formation in adult plant tissues following silencing *ISE1* and *ISE2*

ise1 and *ise2* mutations are embryonic lethal, precluding the analysis of gene function in adult plant tissues. We therefore adopted virus-induced gene silencing (VIGS) as a strategy for investigating *ISE1* and *ISE2* function in *Nicotiana benthamiana* plants. We determined the full-length sequences of *N. benthamiana ISE1* [8] and *ISE2* (Fig. S2) homologs. For VIGS we used *Tobacco rattle virus* (TRV)-based vectors [9,10] containing fragments of *NbISE1*, *NbISE2* or both. The efficiency of silencing *ISE1* and *ISE2* transcripts was 80% (Fig. S3). *ISE1* and/or *ISE2* silenced plants displayed chlorosis but no other developmental or growth abnormalities (Fig. S3).

Twinned and branched PD are often intermediates in the formation of new secondary PD close to existing ones [11,12]. We hypothesized that the T/B PD observed in mutant embryos are secondary and differ in origin from PD in WT embryos. Leaves are a source of accessible cell walls that allow us to investigate the relationship between PD origin, structure and function. *Nicotiana* leaf epidermal cells result from anticlinal divisions in the L1 layer of the shoot apical meristem [13,14]. In young sink leaves PD connecting epidermal cells are mostly primary PD, while all PD connecting epidermal cells to their underlying mesophyll cells are secondary PD [15]. While some reports refer to all branched PD as secondary without assessing their origin ([15] and references therein), here we specifically analyze PD of different origins, either primary or secondary.

We used *ISE1* and/or *ISE2*-silenced *N. benthamiana* plants to measure the distribution of simple or T/B PD in the cell walls connecting epidermal-epidermal or epidermal-mesophyll cells (Fig. 2A) in at least 40 cells in three independent experiments (Table S2). Figure S4 shows the quality of the TEM samples. We limited our analysis to epidermal pavement cells because these cells should have similar function. We excluded trichome cells since they sometimes exhibit periclinal divisions [13] and stomatal guard cells whose function is highly specialized. At 14 dpi the youngest leaves (Leaf 11 Fig. S3) displaying the VIGS phenotype are less that 4mm long and are photosynthetic sinks [5].

Reduced ISE1 or *ISE2* expression does not significantly affect T/B PD formation between epidermal cells

The frequency of PD, 2.5 to 3.2 μm^{-2} epidermal-epidermal cell wall is virtually unchanged in all silenced plants compared to non-silenced controls (Fig. 2B). T/B-PD formation increases to 31% in *ISE2*-silenced plants, albeit this increase is not significant compared to 23% in non-silenced controls (Fig. 2C); this increase in T/B formation is consistent with the increase observed in *ise2* mutant embryos (Fig. 1 and [7]). *ISE1*-silenced tissues do not display a similar increase in T/B-PD formation, and the percentage of T/B PD formed in *ISE1* and *ISE2* double-silenced tissue is more similar to the *ISE1*-silenced samples than the *ISE2*-silenced ones (Fig. 2C).

Reduced *ISE1* or *ISE2* expression significantly increases secondary PD formation between epidermal and mesophyll cells

Silencing *ISE1* results in a statistically significant increase in secondary PD frequency to 3.7 PD μm^{-2} compared to 1.5 PD μm^{-2} in non-silenced control tissues (Fig. 2B). Silencing *ISE2* also increases secondary PD density to 2.35 PD um^{-2}. Silencing *ISE1* and *ISE2* simultaneously has a similar effect to silencing *ISE1* alone resulting in 3.2 PD μm^{-2}.

The formation of T/B PD at epidermal-mesophyll cell-wall junctions increases significantly from 8.5% in control tissues to 35% in *ISE2*-silenced tissues (Fig. 2C). Thus, silencing *ISE2* increases T/B PD formation in both epidermal-epidermal and epidermal-mesophyll cell walls. Silencing of *ISE1* also increases the percentage of T/B secondary epidermal-mesophyll PD to over 20%. Double-silenced tissues also increase T/B PD formation to 13% T/B PD, closer to the values observed for *ISE1* than *ISE2* silencing (Fig. 2C). Thus, without WT ISE1 and ISE2 functions, secondary PD formation increases.

Intercellular movement increases in *ISE1* and/or *ISE2*-silenced plants

ISE1 and/or *ISE2*-silenced *N. benthamiana* plants allow us to use *Tobacco mosaic virus* (TMV) movement protein P30 to probe intercellular movement in leaves. P30 tagged with two tandem copies of GFP (P30-2XGFP) moves cell-to-cell and marks PD as fluorescent punctae in all cells to which it moves [8,16,17]. In contrast 2XGFP moves cell-to-cell by diffusion, does not target to PD, and labels the cytoplasm and nuclei [17]. P30-2XGFP is detected as bright fluorescence in the cytoplasm of the original transformed cell and as punctae in the cell wall when it associates with PD (Fig. 3). In non-silenced leaves by 48 hours post infiltration (hpi) P30-2XGFP moves out of the transformed and into adjacent cells, and by 72 hpi P30-2XGFP moves into more cells (Fig. 3A versus 3B). P30-2XGFP sometimes moves to the underlying mesophyll cells (Fig. 3C-E). We define the original MP30-2XGFP-expressing cell and its surrounding cells containing MP30-2XGFP as a focus.

We infiltrated upper leaves on silenced plants (Leaf 8 or 9, Fig. S3) with *Agrobacterium* carrying 35S::*P30-2XGFP* or 35S::*2XGFP* expression cassettes [8] and monitored their expression and cell-to-cell movement by confocal laser scanning fluorescence microscopy. At 48 hpi in non-silenced controls 13% of foci are 3 or more rings-of-cells wide, compared to 30% of foci in *ISE1*-silenced leaves (Fig. 4A). At 72 hpi 33% of foci are 3 or more rings-of-cells wide in non-silenced leaves compared to 78% in *ISE1*-silenced leaves (Fig. 4B). We also scored P30-2XGFP foci in mesophyll cells. At 48 hpi, 10% of foci in non-silenced leaves display mesophyll P30-2XGFP and this increases to 35% by 72 hpi (Fig. 4C-D). In *ISE1*-silenced plants at 48 and 72 hpi more foci contain P30-2XGFP in the mesophyll, 25% and 50% of foci respectively (Fig. 4 C and D). These results confirm and extend our initial findings of increased MP30-2XGFP movement in *ISE1*-silenced leaves [8]. The same trend of increased cell-to-cell movement in *ISE1*-silenced tissue compared to non-silenced controls was observed with 2XGFP (Fig. 3F versus 3G). However, it is more difficult to monitor 2XGFP movement

past the first ring of cells due to reduced fluorescence intensity on cell-to-cell diffusion of the probe. Figure 4 therefore presents our analyses of P30-2XGFP movement that marks cell walls with punctae.

At 48 hpi 33% of foci in *ISE2*-silenced leaves are 3 or more rings-of-cells wide, compared to 13% in non-silenced leaves (Fig. 4A). By 72 hpi the fraction of foci 3 or more rings-of-cells wide in *ISE2*-silenced tissues was more similar to that observed in control leaves, 44% and 33% respectively (Fig. 4B). Remarkably, the *ISE2*-silenced leaves exhibit a dramatic accumulation of P30-2XGFP in mesophyll PD (Figure 4C-D, Movies S1 and S2). At 48 hpi 35 % of foci contain P30-2XGFP in mesophyll cells, a significant increase over the 10% in non-silenced control leaves. Thus loss of ISE2 causes increased transport of P30-2XGFP, especially by secondary PD.

ISE1-ISE2 double-silenced leaves display a pattern of P30-2XGFP cell-to-cell movement that is more similar to *ISE1*-silenced plants than to *ISE2*-silenced ones (Fig. 4). These latter data are consistent with the results in Figure 2, where the effects on PD frequency or fraction T/B PD in double-silenced plants are more similar to those produced by silencing *ISE1* than *ISE2*.

Conclusions

The production of secondary PD in *Arabidopsis* embryogenesis is genetically controlled, and ISE1 and ISE2 are crucial to this process. ISE1 and ISE2 also control secondary PD formation in immature, sink leaves in *N. benthamiana*. Thus, the increased intercellular transport observed upon loss of ISE1 or ISE2 occurs via secondary PD. ISE1 and ISE2 are the first proteins described to influence *de novo* formation of PD. The mutants and silencing system described here provide a novel system for investigating the regulatory pathways controlling the formation of secondary PD. What roles could ISE1 and ISE2 play in secondary PD formation? ISE1 is a mitochondrial DEAD-box RNA helicase [8]. ISE1 may influence secondary PD formation by modulating cellular energy status. ISE2 is a DEVH RNA helicase [7]. Its localization to cytoplasmic granules [7] and homology to Ski2 proteins [18] suggest that reduced ISE2 may disrupt processing of mRNAs encoding proteins involved in the regulation or production of secondary PD formation. Thus, two distinct critical cellular pathways affect PD synthesis.

Experimental Procedures

Transmission Electron Microscopy of *Arabidopsis* embryos

Arabidopsis plants were grown in growth chambers under long-day conditions (16h light and 8h darkness) at 24°C. Mutant and sibling WT embryos (Figure S1) were collected, high-pressure frozen, freeze-substituted in OsO_4 according to [7], and prepared for TEM (Supplementary Materials). PD structure was examined in the entire cotyledon or hypocotyl of 2 or more non-serial longitudinal sections for each genotype covering approximately the same cell wall-length in each sample of a given stage, to obtain the data presented in Table S1. ss

Virus-induced Gene Silencing and microscopy

pTBS16 [8] was used to silence *ISE1*. To silence *ISE2*, an *NbISE2* fragment was amplified from *N. benthamiana* cDNA (See Supplementary Materials) and cloned into pTRV1 (pYL156, [9]) by restriction digest and ligation to generate pTBS13. To co-silence *ISE1* and *ISE2*, the fragment for NbISE1 silencing was introduced into pTBS13 by restriction digest and ligation to produce the double-silencing construct pSH2. Silencing constructs were introduced into

Agrobacterium strain GV3101 for plant infiltrations. *N. benthamiana* plants were grown under continuous light. VIGS was performed on three week-old plants according to [19] and Supplementary Materials. VIGS experiments were performed at least four times, using four plants for each sample per experiment.

Upper leaves displaying the silencing phenotype were infiltrated with *Agrobacterium* containing constructs encoding P30-2XGFP or 2XGFP two weeks after VIGS induction. Leaf samples were examined 48 or 72 hours later by confocal laser scanning microscopy (Zeiss LSM 510 with Meta detector (Carl Zeiss Inc., Jena, Germany)). At least 40 P30-2XGFP foci were imaged for each silenced gene over three or more experiments.

For TEM disks were cut from the youngest leaves (Leaf 11, Fig.S3) showing the silencing phenotype, avoiding vascular tissue, and samples were prepared for TEM (See Supplementary Materials). For each sample three or more sections, each from a separate VIGS experiment, was examined. Only PD traversing at least half the wall between two cells were scored. The density of PD μm^{-2}, F, was calculated after [20]. Briefly, F= count per μm of wall length / (T + 1.5R), where T = section thickness in μm and R = radius of the outermost dimension of the PD (μm). In our system T= 60 nm (0.06 μm) and we assumed R= 25 nm (0.025 μm) based on our TEM images.

Statistical analysis

We used the Wilcoxon rank-sum test for non-parametric data using R (http://www.r-project.org/) and Z-ratios to test if differences in the proportions of T/B PD were significant.

Supplementary Material

Refer to Web version on PubMed Central for supplementary material.

Acknowledgments

We thank Dr. Marisa Otegui (University of Wisconsin) for preparation of *Arabidopsis* embryos for TEM, Dr. Kent McDonald and Reena Zalpuri for assistance with TEM, and Dr. Erick Matsen for help with statistical analysis. We thank Dr. S.P. Dinesh-Kumar (Yale University) for TRV silencing plasmids and *N. benthamiana* seeds. TBS is supported by a post-doctoral fellowship from the UCB Miller Institute for Basic Research in Science. PD research in the Zambryski lab is funded by the National Institutes of Health grant GM45244.

References

1. Cilia ML, J D. Plasmodesmata form and function. Current Opinion in Cell Biology 2004;16:500–506. [PubMed: 15363799]
2. Lucas WJ, Lee JY. Plasmodesmata as a supracellular control network in plants. Nat Rev Mol Cell Biol 2004;5:712–726. [PubMed: 15340379]
3. Kim JY. Regulation of short-distance transport of RNA and protein. Curr Opin Plant Biol 2005;8:45–52. [PubMed: 15653399]
4. Zhu T, O'Quinn RL, Lucas WJ, Rost TL. Directional cell-to-cell communication in the Arabidopsis root apical meristem II. Dynamics of plasmodesmatal formation. Protoplasma 1998;204:84–93.
5. Oparka KJ, Roberts AG, Boevink P, Santa Cruz S, Roberts I, Pradel KS, Imlau A, Kotlizky G, Sauer N, Epel B. Simple, but not branched, plasmodesmata allow the nonspecific trafficking of proteins in developing tobacco leaves. Cell 1999;97:743–754. [PubMed: 10380926]
6. Kim I, Hempel FD, Sha K, Pfluger J, Zambryski PC. Identification of a developmental transition in plasmodesmatal function during embryogenesis in Arabidopsis thaliana. Development 2002;129:1261–1272. [PubMed: 11874921]

7. Kobayashi K, Otegui MS, Krishnakumar S, Mindrinos M, Zambryski P. INCREASED SIZE EXCLUSION LIMIT 2 encodes a putative DEVH box RNA helicase involved in plasmodesmata function during Arabidopsis embryogenesis. Plant Cell 2007;19:1885–1897. [PubMed: 17601829]
8. Stonebloom S, Burch-Smith T, Kim I, Meinke D, Mindrinos M, Zambryski P. Loss of the plant DEAD-box protein ISE1 leads to defective mitochondria and increased cell-to-cell transport via plasmodesmata. Proc Natl Acad Sci U S A 2009;106:17229–17234. [PubMed: 19805190]
9. Liu Y, Schiff M, Marathe R, Dinesh-Kumar SP. Tobacco Rar1, EDS1 and NPR1/NIM1 like genes are required for N-mediated resistance to tobacco mosaic virus. Plant J 2002;30:415–429. [PubMed: 12028572]
10. Burch-Smith TM, Anderson JC, Martin GB, Dinesh-Kumar SP. Applications and advantages of virus-induced gene silencing for gene function studies in plants. Plant J 2004;39:734–746. [PubMed: 15315635]
11. Faulkner C, Akman OE, Bell K, Jeffree C, Oparka K. Peeking into pit fields: a multiple twinning model of secondary plasmodesmata formation in tobacco. Plant Cell 2008;20:1504–1518. [PubMed: 18667640]
12. Ehlers K, van Bel AJ. Dynamics of plasmodesmal connectivity in successive interfaces of the cambial zone. Planta 2010;231:371–385. [PubMed: 19936780]
13. Stewart RN, Burk LG. Independence of tissues derived from apical layers in ontogeny of the toabcco leaf and ovary. American Journal of Botany 1970;57:1010–1016.
14. Marcotrigiano M. Genetic mosaics and the analysis of leaf development. International Journal of Plant Sciences 2001;162:513–525.
15. Ehlers K, Kollmann R. Primary and secondary plasmodesmata: structure, origin, and functioning. Protoplasma 2001;216:1–30. [PubMed: 11732191]
16. Kim I, Kobayashi K, Cho E, Zambryski PC. Subdomains for transport via plasmodesmata corresponding to the apical-basal axis are established during Arabidopsis embryogenesis. Proc Natl Acad Sci U S A 2005;102:11945–11950. [PubMed: 16087887]
17. Crawford KM, Zambryski PC. Subcellular localization determines the availability of non-targeted proteins to plasmodesmatal transport. Curr Biol 2000;10:1032–1040. [PubMed: 10996070]
18. Linder P, Owttrim GW. Plant RNA helicases: linking aberrant and silencing RNA. Trends Plant Sci 2009;14:344–352. [PubMed: 19446493]
19. Liu Y, Burch-Smith T, Schiff M, Feng S, Dinesh-Kumar SP. Molecular chaperone Hsp90 associates with resistance protein N and its signaling proteins SGT1 and Rar1 to modulate an innate immune response in plants. J Biol Chem 2004;279:2101–2108. [PubMed: 14583611]
20. Robards, AW. Plasmodesmata in Higher Plants. In: Gunning, BES.; Robards, AW., editors. Intercellular Comminucation in Plants: Studies on Plasmodesmata. Heidelburg: Springer-Verlag Berlin Heidelburg New York; 1976. p. 15-57.

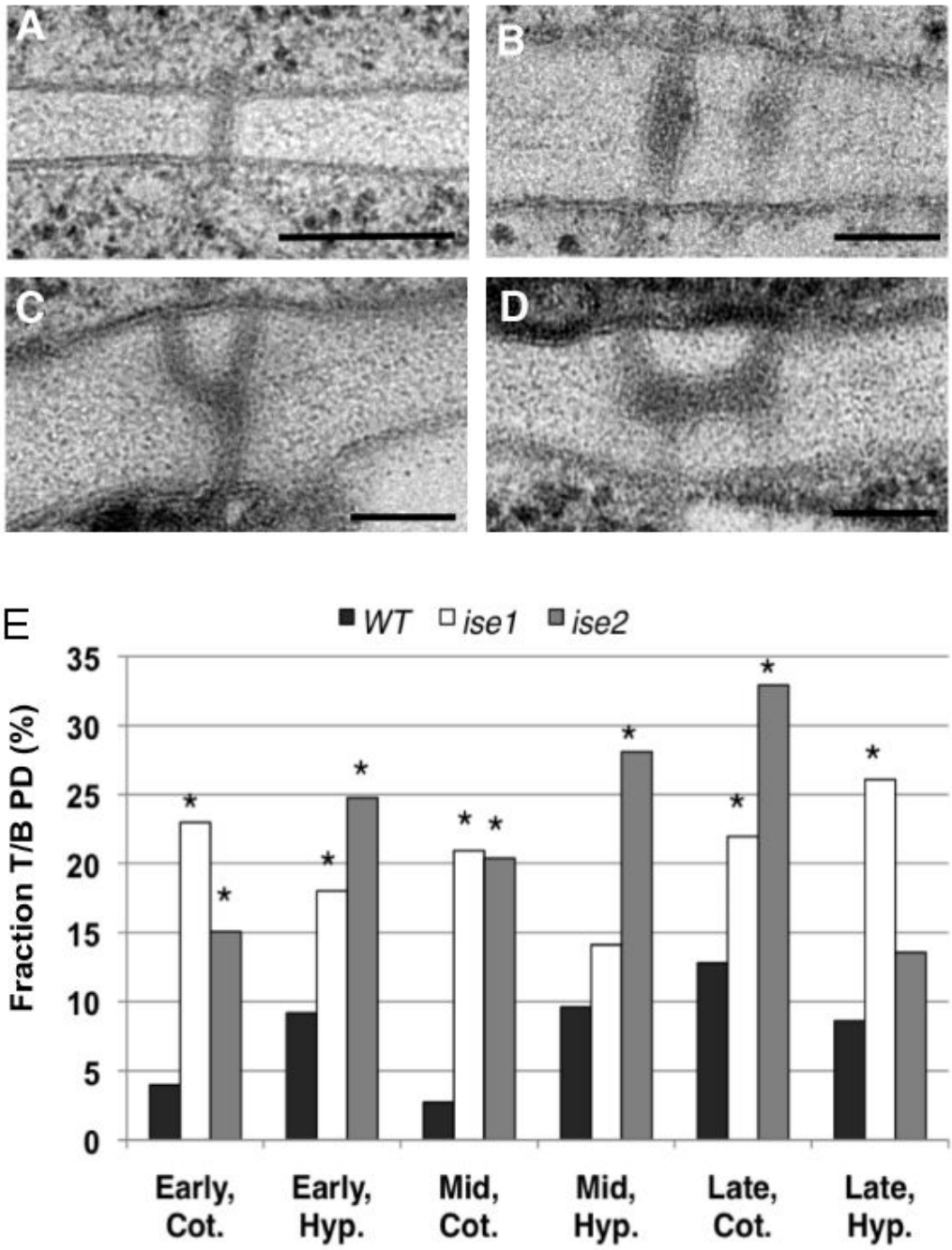

Figure 1. Analysis of PD structure in embryonic cotyledons and hypocotyls

(A) Simple PD. (B) Twinned PD. (C-D) Branched PD may be Y or H-shaped. Scale bar represents 200 nm in (A) and 100 nm in (B, C and D).

(E) The fraction of twinned and branched (T/B) PD were counted in cotyledons and hypocotyls from early-, mid-, and late-torpedo embyos. *$p<0.05$ compared to wild type tissues. Refer to Figure S1.

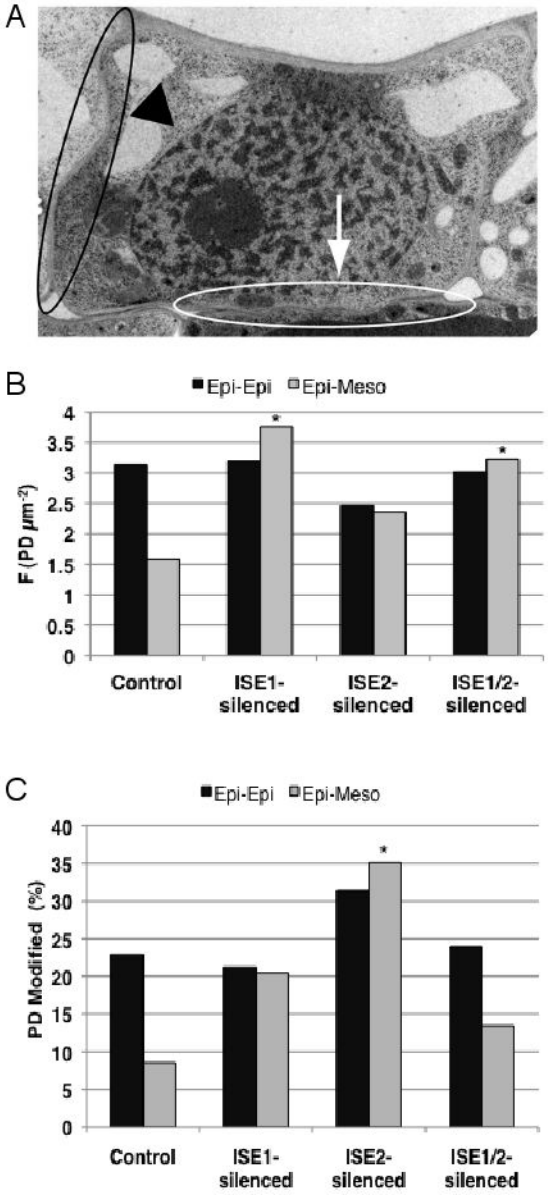

Figure 2. Frequency of PD per um^2 and T/B PD formed in *N. benthamiana* cell walls

(A) Representative TEM image of an epidermal cell from the youngest leaf. Left, epidermal-epidermal cell wall (arrowhead). Bottom, epidermal-mesophyll cell wall (arrow).

(B) Mean PD frequency um^{-2} in epidermal-epidermal (black bars) or epidermal-mesophyll (grey bars) cell walls. *$p<0.05$ compared to non-silenced control leaves.

(C) Proportions of T/B PD in epidermal-epidermal (black bars) and epidermal-mesophyll (grey bars) cell walls. *$p<0.05$ compared to non-silenced control leaves.

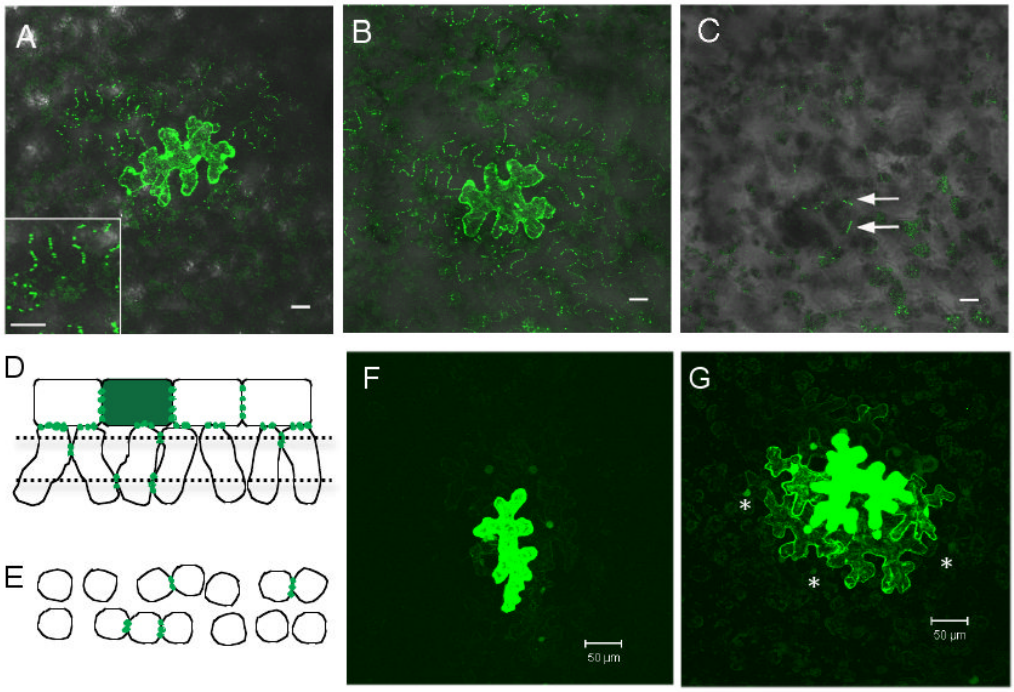

Figure 3. P30-2XGFP and 2XGFP cell-to-cell transport via PD

(A-B) Z-series projections from non-silenced *N. benthamiana* leaf tissue 48 hpi (A) or 72 hpi (B) with *Agrobacterium* carrying the P30-2XGFP expression cassette. The brightest cell is the primary transformed cell and the surrounding cells are cells into which the P30-2XGFP has moved via PD. P30-2XGFP marks PD as bright punctae (inset).

(C) Mesophyll cells under the focus in (B) contain P30-2XGFP. Arrows, mesophyll cell walls containing P30-2XGFP.

(D) Cartoon of side view of P30-2XGFP foci. The primary transformed cell is bright green. P30-2XGFP moves cell-to-cell and localizes to PD (green punctae) of neighbouring epidermal cells and mesophyll cells below. Dotted lines represent cross-section planes for cells shown in top-down view in (E).

(E) Cartoon of top-down view of cross-section of mesophyll cells in (D). P30-2XGFP punctae in PD (green punctae), as observed in (C).

(F) Z-stack projection through a 2XGFP focus in a non-silenced leaf at 72 hpi. Bright cell is the primary, transformed cell where GFP localizes throughout the cell. Low 2XGFP fluorescence occurs in the cytoplasm and nuclei of the surrounding ring of cells.

(G) Z-stack projection through a 2XGFP focus in an *ISE1*-silenced *N. benthamiana* leaf at 72 hpi. 2XGFP moves extensively into the neighboring 2 rings of cells. There is a gradient of GFP fluorescence from the primary cell to the second ring of cells. Asterisks mark the nuclei of the second ring of cells.

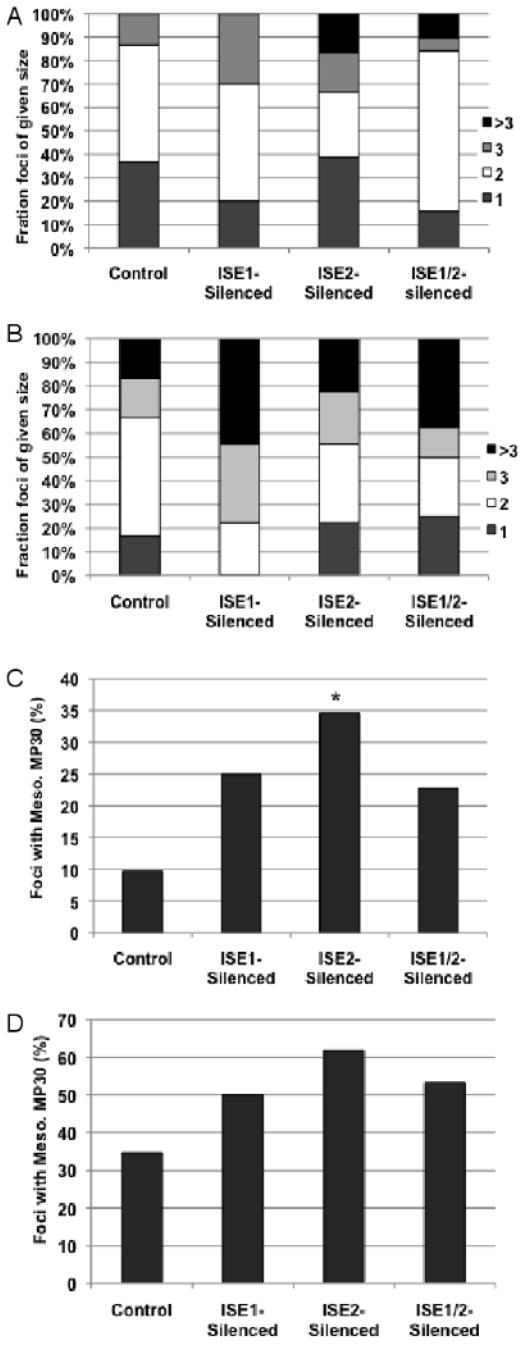

Figure 4. Cell-to-cell transport is altered in *ISE1* and/or *ISE2*-silenced leaves

(A) Size of foci measured as numbers of rings of cells containing P30-2XGFP punctae around a transformed cell 48 hpi in control or silenced leaves.

(B) Size of P30-2XGFP foci at 72 hpi in control or silenced leaves.

(C) Number of foci with P30-2XGFP in the mesophyll PD at 48 hpi scored as a percent of the total number of foci observed. *p <0.05 compared to non-silenced controls.

(D) Fraction of foci with P30-2XGFP in the mesophyll PD at 72 hpi.